Preprints of the 19th World Congress
The International Federation of Automatic Control
Cape Town, South Africa. August 24-29, 2014

ROBUST MODEL-BASED SOFT SENSOR: DESIGN AND APPLICATION

Rajamani Doraiswami*, and Lahouari Cheded**

*Department of Electrical and Computer Engineering, University of New Brunswick, Fredericton, New Brunswick, Canada.
**Systems Eng. Department, King Fahd University of Petroleum & Minerals, Dhahran 31261, KSA,

Abstract: A model-based robust soft sensor is proposed here. The soft sensor is based on a Kalman filter (KF), which is designed to estimate the inaccessible variables using the output measurements in the face of the measurement noise, disturbances, and model perturbations. The performance of the soft sensor critically depends upon the reliability and accuracy of the identified system model it is based on. To overcome the degradation due to model mismatch, a reliable offline identification scheme, based on the powerful concept of emulator which significantly improved the accuracy of the proposed scheme, is proposed here. It involves performing a number of experiments using emulators, which are transfer function blocks connected to the system input or the output, and which are used to introduce model perturbations to mimic likely operating scenarios. It is shown that the KF residual is a function of the product of the model perturbation and the control input sensitivity function. The proposed new soft sensor is successfully evaluated on a simulated and laboratory-scale physical velocity control system.

Keywords: Soft Sensing, Dynamic Modeling, Kalman Filtering, Subspace Identification, DC Servo motor Control, Emulators, Status Monitoring, Velocity Control

1. INTRODUCTION

A soft sensor can be broadly defined as a software-based sensor, and are used in industrial applications to replace hardware sensors, which are costly, difficulty to maintain, and even impossible to physically access. Soft sensors are maintenance-free and play additional role in numerous applications such as fault diagnosis, fault-tolerant control systems, and quality control, aerospace, pharmaceutical, and process control, mining, oil and gas, and healthcare industries (Fortuna, Graziani, & Xibilia, 2007), (Kadlec, Gabrys, & S, 2009). It is anticipated that the wave of soft sensing will sweep through the measurement world through its increasing use in smart phones nowadays. Soft sensing is already providing the core component of the new and emerging area of smart sensing. The design and use of a soft sensor is illustrated in this paper in the specific and important area of robust and fault-tolerant control.

A soft sensor uses a software algorithm that derives its sensing power from the use of an Artificial Neural networks, a Neuro-fuzzy system, Kernel methods (support vector machines), a multivariate statistical analysis, a Kalman filter or other model-based or model-free approaches (Angelov & Kordon, 2010). A model-based approach using a Kalman filter for the design of a soft sensor is proposed here.

1.1 Soft sensor

The Kalman filter estimates unmeasured or inaccessible variables. It is an optimal minimum-variance estimator of the unknown variable from the noisy input and output of the system. The estimate is computed by fusing the *a-posteriori* information provided by the measurement, and the *a-priori* information contained in the model that generated the measurement, and is thus the best compromise between the estimates generated by the model (i.e. the predicted estimates) and those obtained from the measurement (i.e. the actual measurements), depending upon the plant noise and the measurement noise covariance.

A Kalman filter is a copy of the mathematical model of the plant driven by the *residual*, which is the error between the measured output of the plant and its estimate generated by the Kalman filter. The Kalman gain is used as an effective design parameter to handle the uncertainty associated with the model of the physical system. Model uncertainty is effectively introduced in the determination of the gain by choosing a variance of the plant noise higher (lower) than the measurement noise variance if the dynamic part of the state-space model is less (more) reliable. In (Doraiswami & Cheded, 2012), an expression relating the KF residual and the deviation of the plant model from its nominal one is derived. This relationship is exploited herein to a) ensure high system performance and stability by re-identifying the plant whenever the residual exceeds some threshold and b) to develop a fault-tolerant system (Doraiswami & Cheded, 2013).

1.2 Reliable Identification of the system

The Kalman filter is designed using the identified nominal model of the system. Hence the performance of the the soft sensor depends critically upon the accuracy of the identified model. In general, a model of the physical system varies with the operating conditions. A model identified at a given operating point may not be accurate when the operating condition changes. This will then result in the degradation of the performance of both the soft sensor and the controller. To overcome this performance degradation, a set of models in the neighbourhood of a given operating point is generated by performing a number of virtual experiments using the powerful tool of emulators. A model termed *optimal nominal model* is identified using the subspace method, which is the optimal fit to the set of models thus obtained. To generate the set of models, emulators are connected at the input or at the output. These neighbouring operating points are determined by varying the parameters of the emulators.

Soft sensors offer several attractive benefits, such as:

Reduced cost and weight:

Reliability: It is maintenance-free and software-based and is devoid of physical accessibility and danger (e.g. nuclear reactors)

Sensing versatility and product quality: It can estimate almost any desired variable and does so with a high accuracy, thus ensuring a high quality of a product (composition, texture, molecular weight, etc.) indirectly using available measurements coupled with a process model

Fusion of Measurements: Soft sensors are especially useful in data fusion, where measurements of different process characteristics and dynamics are combined to generate measurement of physical variables that may be inaccessible to hardware sensors.

Process estimators and controllers: It can be used for performance monitoring, fault diagnosis, as well as for implementing a controller estimating unmeasured plant outputs.

The proposed scheme has been successfully evaluated on both a simulated and physical DC servomotor.

2. MATHEMATICAL FORMULATIONS

The state-space model of a system is given by:

$$\begin{aligned} \boldsymbol{x}(k+1) &= \boldsymbol{A}\boldsymbol{x}(k) + \boldsymbol{B}u(k) + \boldsymbol{E}_w w(k) \\ \boldsymbol{y}(k) &= \boldsymbol{C}\boldsymbol{x}(k) + \boldsymbol{F}_v v(k) \\ y_r(k) &= \boldsymbol{C}_r \boldsymbol{x}(k) \end{aligned} \quad (1)$$

where $x(k)$ is a $nx1$ state, $u(k)$ the scalar control input , $\boldsymbol{y}(k)$ a $n_y x1$ vector formed of all measured (accessible) outputs, v a measurement noise, w a disturbance, $y_r(k)$ the plant output that needs to be estimated as it is either inaccessible or unmeasurable, $\boldsymbol{A}$, $\boldsymbol{B}$, $\boldsymbol{C}$ and $\boldsymbol{C}_r$ are respectively nxn , $nx1$, $n_y xn$ and $1xn$ matrices, and v , w and y_r are scalars; $\boldsymbol{E}_w$ and $\boldsymbol{F}_v$ are, respectively, the $nx1$ disturbance and the $n_y x1$ measurement noise entry vectors. The measurement noise v and disturbances are zero-mean white noise with variances *Q* and *R* respectively.

2.1 Transfer function model

The transfer function model of the system relating the reference input $r(z)$, the disturbance $\boldsymbol{w}(z)$ and the measurement noise $\boldsymbol{v}(z)$ to the output $\boldsymbol{y}(z)$ is given by:

$$\boldsymbol{y}(z) = \frac{\boldsymbol{N}(z)}{D(z)}u(z) + \frac{\boldsymbol{N}_w(z)}{D(z)}\boldsymbol{w}(z) + \boldsymbol{F}_v \boldsymbol{v}(z) \quad (2)$$

where $\boldsymbol{G}(z) = \frac{\boldsymbol{N}(z)}{D(z)} = \boldsymbol{C}(zI - \boldsymbol{A})^{-1}\boldsymbol{B}$, $\frac{\boldsymbol{N}_w(z)}{D(z)} = \boldsymbol{C}(zI - \boldsymbol{A})^{-1}\boldsymbol{E}_w$ are $n_y x1$ transfer matrices, and $D(z) = |\boldsymbol{I}z - \boldsymbol{A}|$ is a scalar. Rewriting (2) by cross-multiplying by $D(z)$, we get:

$$D(z)\boldsymbol{y}(z) = \boldsymbol{N}(z)u(z) + \boldsymbol{\upsilon}(z) \quad (3)$$

where $\boldsymbol{\upsilon}(z) = \boldsymbol{N}_w(z)\boldsymbol{w}(z) + D(z)\boldsymbol{F}_v\boldsymbol{v}(z)$ is the equation error formed of two colored noise processes generated by the disturbance $\boldsymbol{w}(z)$ and the measurement noise $v(z)$.

2.2 Uncertainty model

The structure and the parameters of a physical system may vary due to changes in the operating regime. The difference between the actual system and its model, termed *model uncertainty*, is considered in identification. Commonly, the transfer function model of the system is expressed as an additive or multiplicative combination of the assumed model and a perturbation term. The perturbation term represents in effect the modelling error. A model, termed the numerator-denominator perturbation model, is employed herein, where the perturbations in the numerator and denominator polynomials are treated separately instead of being clubbed together as a single perturbation term in the overall transfer function (Kwakernaak, 1993). The numerator-denominator perturbation model (Kwakernaak, 1993) takes the following form:

$$\boldsymbol{G}(z) = \boldsymbol{G}_e(z)\boldsymbol{G}_0(z) \quad (4)$$

where $\boldsymbol{G}_0(z) = \frac{\boldsymbol{N}_0(z)}{D_0(z)}$ is the nominal transfer function, $\boldsymbol{N}_0(z)$ is the nominal numerator (matrix) polynomial, $D_0(z)$ the nominal denominator (scalar) polynomial, and $\boldsymbol{G}_e(z)$ the $n_y xn_y$ multiplicative perturbation, termed here as the *emulator*

$$\boldsymbol{G}_e(z) = \frac{\boldsymbol{I} + \Delta_N(z)}{1 + \Delta_D(z)} \quad (5)$$

$\Delta_N(z) \in RH_\infty$ and $\Delta_D(z) \in RH_\infty$ represent, respectively, the pertutbations in the numerator and denominator polynomials of the nominal model $\boldsymbol{G}_0(z)$, $\Delta_N(z)$ and $\Delta_D(z)$ are respectively, a stable frequency-dependent $n_y xn_y$ matrix, and a scalar; $\boldsymbol{I}$ is an $n_y xn_y$ identity matrix.

2.3 Selection of the emulator model

The emulator $\boldsymbol{G}_e(z)$ is chosen such that the perturbed model $\boldsymbol{G}(z)$ matches the actual model of the system. In many practical problems, for computational simplicity, the perturbation model is chosen to mimic the macroscopic behaviour of the system characterized by gain and phase changes in the system transfer function. The $n_y xn_y$ multiplicative perturbation $\boldsymbol{G}_e(z)$ is a diagonal matrix:

$$\boldsymbol{G}_e(z) = diag\left[G_{e1}(z) \quad G_{e2}(z) \quad . \quad G_{en_y}(z)\right] \quad (6)$$

where $G_{ei}(z)$ is chosen to be a constant gain (γ_i), a gain and a pure delay of d time instants ($\gamma_i z^{-d}$), an all-pass first-order filter ($\gamma_i \frac{\gamma_i + z^{-1}}{1 + \gamma_i z^{-1}}$) or a Blaschke product of all-pass first-order filters ($\gamma_i \prod_j \frac{\gamma_{ij} + z^{-1}}{1 + \gamma_{ij} z^{-1}}$), where γ_i , and γ_{ij} are termed herein as the *emulator* parameters.

3. IDENTIFICATION OF THE SYSTEM

The output $y_r(k)$ is considered here either inaccessible or not measurable during the operational phase of the system. However, during the offline identification phase, the output $y_r(k)$ is either measured (for example the angular velocity may be measured using a physical tachometer) or computed from other outputs. The direct or indirect availability of the measured value of $y_r(k)$ will ensure that, during the identification phase, the identified model will capture accurately the map relating $y_r(k)$ to the input $u(k)$ and the measured output $\boldsymbol{y}(k)$. In the other words, during offline identification, it is assumed that $y_r(k)$ is an element of the measured output vector $\boldsymbol{y}(k)$. For notational simplicity, whenever there is no confusion the augmented and the measured outputs are denoted by the same output variable $\boldsymbol{y}(k)$.

3.1 Perturbed-parameter experiments

The performance of the soft sensor depends upon the accuracy of the identified nominal model, which is used to design the Kalman filter. To ensure this accuracy, a reliable identification scheme is employed here. The system model is identified by performing a number of parameter-perturbed experiments. Each experiment consists of perturbing one or more emulator parameters. The input is chosen to be persistently exciting to allow the model to capture as much as possible of the system dynamics. We can emulate an operating scenario by including the emulator $G_{ej}(z)$ at the input of the system $u(k)$, and varying the emulator parameters γ_i, and γ_{ij} as shown in the Fig. 1, (Doraiswami & Cheded, 2013). The use of the emulator entails carrying out all the necessary experiments which consist of perturbing, one-at-a-time, all the parameters of the emulator $\boldsymbol{G}_e(z)$, and collecting both the input data $u(k)$ (usually the input is chosen to be same for all experiments), and the output $y(k)$. Consider the j^{th} experiment of perturbing the j^{th} emulator parameter. The perturbed model of the system obtained using (4) , which relates the i^{th} output $y_i(z)$, the input $u(z)$ and the i^{th} equation error $\upsilon_i(z)$, then becomes:

$$D^j(z)y_i^j(z) = N_i^j(z)u(z) + \upsilon_i^j(z) \tag{7}$$

where $D^j(z)$ and $N_i^j(z)$ aree the denominator and numerator polynomials, respectively, resulting from the variation of the j^{th} emulator parameter.

3.2 Optimal nominal model

The objective here is to find an *optimal nominal model* whose input-output data set is a best fit to those similar data sets generated from the parameter-perturbed experiments to mimic the operating scenarios of the actual system. The input-output data from the experiments given by (7) are collected and a model that is a best fit to data is then identified. Let $\boldsymbol{y}^0(k)$ be an $n_y n_{\exp} x1$ vector of $n_y x1$ outputs $\{\boldsymbol{y}^j(k)\}$ collected from all experiments, $j = 1,2,3,...,n_{\exp}$, that is given by: $\boldsymbol{y}^0(k) = \left[\left(\boldsymbol{y}^1(k)\right)^T \quad \left(\boldsymbol{y}^2(k)\right)^T ... \quad \left(\boldsymbol{y}^{n\exp}(k)\right)^T\right]^T$, where $\boldsymbol{y}^j(k) = \left[y_1^j \quad y_2^j \quad\quad y_{n_y}^j\right]^T$ is the $n_y x1$ output from the j^{th} experiment. Now let $\hat{\boldsymbol{y}}^0(k)$ be the output of the optimal model subjected to the same input $\left(\boldsymbol{A}_{p0}, \boldsymbol{B}_{p0}, \boldsymbol{C}_{p0}\right)$.Our objective here is to find an *optimal nominal model* such that $\hat{\boldsymbol{y}}^0(k)$ is close to $\boldsymbol{y}^0(k)$ in some optimal sense, for example such that the norm $\left\|\boldsymbol{y}^0(k) - \hat{\boldsymbol{y}}^0(k)\right\|^2$ is minimum. Since the soft sensor is a Kalman filter, it is preferable that the optimal nominal model be identified in a state-space form.

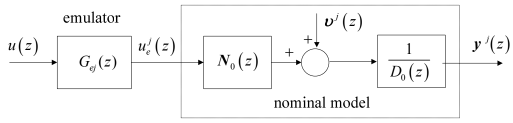

Fig.1 Emulation of operating scenarios

3.3 Subspace identification

The subspace identification has received a lot of attention in recent years, as it is numerically efficient and robust, and requires minimal a-priori information such as the structure of the system, i.e. the model order of the numerator and the denominator polynomials and the delay (Qin, 2006), (Wahlberg, Jansson, Matsko, & Molander, 2007). The only design parameter is the threshold value for the truncation the singular values required in the subspace identification method. This method estimates directly the state-space model for the system and is well suited for application including Kalman filtering. However, although the identified state-space model is *similar* to that of the system (i.e. the rank, the eigenvalues, the determinant and the trace are all identical), the states of the system and those associated with the identified model may not have the same physical meaning. It is easier for a practitioner to implement this scheme as there are only a few design parameters to choose. The subspacealgorithm does not require non-linear searches in the parameter space and is based on computationally-reliable tools such as the SVD. Subspace identification is non-recursive, is based on robust SVD-based numerical methods and avoids problems associated with optimization and possible local minima. The model order selection process is a simple one and is based merely on truncating the 'low singular values' of the estimated Hankel matrix. Two versions of the subspace method, namely the prediction and the innovation forms are given here. The prediction and the innovation forms use respectively, the predictor model structure and the innovation model structure of the Kalman filter. The predictor form is numerically stable when the system model is poorly damped or the system is close to be unstable.

Given the input $u(k)$ and the output $\boldsymbol{y}^0(k)$, the subspace method identifies directly the state-space model denoted by $(\boldsymbol{A}_0, \boldsymbol{B}_0, \boldsymbol{C}_0)$, and the Kalman gain $\boldsymbol{K}$. The model order n is also estimated. The identified model is given by

$$\begin{aligned} \boldsymbol{x}(k+1) &= \boldsymbol{A}_0\boldsymbol{x}(k) + \boldsymbol{B}_0 u(k) \\ \boldsymbol{y}(k) &= \boldsymbol{C}_0\boldsymbol{x}(k) \\ y_r(k) &= \boldsymbol{C}_{r0}\boldsymbol{x}(k) \end{aligned} \tag{8}$$

Assumptions: It is assumed that $(\boldsymbol{A}_0, \boldsymbol{B}_0)$ is controllable and $(\boldsymbol{A}_0, \boldsymbol{C}_0)$ are both observable, so that a controller and a (steady state) Kalman filter may be designed to meet the requirement of performance and stability.
For notation simplicity the state space of the actual, the nominal and the identified nominal models is indicated by the same state $\boldsymbol{x}(k)$.

3.4 Illustrative example
A simple example of a second-order system is considered here for illustration purposes.
The nominal model of the system $G_0(z)$ is:

$$G_0(z) = \frac{N_0(z)}{D_0(z)} = \frac{b_{01}z^{-1}}{1 + a_{01}z^{-1}} \qquad (9)$$

The emulator model $G_e(z)$ is:

$$G_e(z) = \frac{1 + \Delta_N(z)}{1 + \Delta_D(z)} = \frac{\gamma + z^{-1}}{1 + \gamma z^{-1}} \qquad (10)$$

where $b_{01} = 1$, $a_{01} = 0.8$, and γ is the emulator parameter, and $\Delta_N(z) = \gamma - 1 + z^{-1}$, $\Delta_D(z) = \gamma z^{-1}$ are the perturbation terms.
The actual model of the system $G(z)$ given by (4) becomes:

$$G(z) = \frac{\gamma + z^{-1}}{1 + \gamma z^{-1}} \frac{b_{01}z^{-1}}{1 + a_{01}z^{-1}} = \frac{b_1 z^{-1} + b_2 z^{-2}}{1 + a_1 z^{-1} + a_2 z^{-2}} \qquad (11)$$

where $b_1 = b_{01}\gamma$, $b_2 = b_{01} = 1$, $a_1 = a_{01} + \gamma = 0.8 + \gamma$, $a_2 = a_{01}\gamma = 0.8\gamma$.
The output of the system $y(z)$ becomes:

$$y(z) = G(z)u(z) + \upsilon(z) \qquad (12)$$

where $b_1 = 0.9$; $b_2 = 1$; $a_1 = 1.7$; $a_2 = 0.72$. The number of data samples is $N = 100$; $\text{var}(\upsilon) = 0.01$, and the input used was a square wave. Ten experiments were performed by varying the emulator parameter γ in the range 0.1 to 1 in equal steps of 0.1. The perturbed model (7) becomes:

$$\left(1 + (a_{10} + \gamma)z^{-1} + a_{10}\gamma z^{-2}\right)y^j(z) = \left(b_{01}\gamma z^{-1} + b_{10}z^{-2}\right)u(z) + \upsilon^j(z) \quad (13)$$

where $\gamma = 1 - 0.1(j-1)$ for $j = 1,2,3,...,10$.
Fig. 2 shows the j^{th}-output $y^j(k)$ and the optimal estimate $\hat{y}^0(k)$ and the identification errors $\sum_{k=1}^{N}\left(y^j(k) - \hat{y}^0(k)\right)^2$ for the proposed scheme and $\sum_{k=1}^{N}\left(y^j(k) - \hat{y}^{j0}(k)\right)^2$ for the conventional one. The top three subfigures A, and B, and C and D show respectively the results of the conventional and the proposed identification approaches. The actual outputs (in dotted lines), and their optimal estimates (in solid lines) are displayed when the chosen emulator parameters are respectively $\gamma = 0.99$,and $\gamma = 0.8$. The bottom subfigure E shows the errors in the identification for the proposed and the conventional cases.

Comment: The proposed identification based on performing a number of emulator parameter perturbed experiments is significantly superior to that of the conventional scheme based on performing a single experiment at a given operating point as shown in Fig. 2. The proposed identified optimal model was able to capture the variation in the system model significantly better. This constitutes one of the major contributions of this paper.

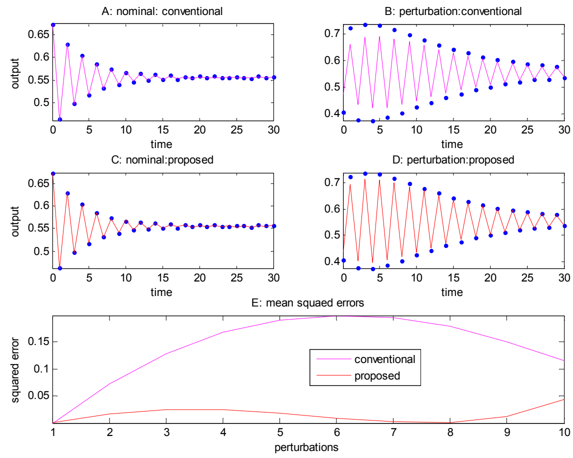

Fig.2 Output, optimal estimate and identification errors

4. MODEL OF THE KALMAN FILTER

There are two approaches to estimate an unmeasured variable, namely an observer and a Kalman filter. The KF is chosen as its performance in the presence of noise and the disturbances are superior: the variance of the residual of the KF is minimum, the auto correlation of the residual of the KF is a zero mean white noise process, which implies the KF has captured all the information about the system model and what is leftover, namely the residual, is information-less random process. These key properties are exploited in developing fault tolerant system. If there is an increase in the variance of the residual and/or a deviation from the white noise type behaviour of the residual, it indicated that there is a fault, a variation in the system nominal model $(\boldsymbol{A}, \boldsymbol{B}, \boldsymbol{C})$.

If there is fault, it is detected, isolated and accommodated. On the other hand if there is no fault, implying that the there is a variation in the model of the system. In this case the Kalman gain $\boldsymbol{K}_0$ is tuned on-line, that is KF is an adaptive filter. In the extreme case of variations, the system is re-identified to obtain a highly accurate nominal using either a hard sensor or some other measurement device. However, these model variations are may be infrequent.

An observer is a simple estimating device and may be used in situations where the signal to noise ratio is large. In this case the KF and the observer are essentially the same.

KF-based soft sensor design: The soft sensor provides the estimate $\hat{y}_r$ of the un-measurable (inaccessible) variable y_r as the output of the KF. Fig. 3 shows the interconnection between the plant and the KF. The inputs to the KF are the control input u and measured outputs of the plant $\boldsymbol{y}$. The KF contains a copy of the model of the plant, which is driven by the residual, an error between the plant output $\boldsymbol{y}$ and its estimate $\hat{\boldsymbol{y}}$. $\boldsymbol{K}_0$ is the Kalman gain which minimizes the covariance of the estimation error $\boldsymbol{e}$.

4.1 Model of the Kalman filter (KF):

The model of the KF is given by:

$$\begin{aligned} \boldsymbol{x}_0(k+1) &= \left(\boldsymbol{A}_0 - \boldsymbol{K}_0\boldsymbol{C}_0\right)\boldsymbol{x}_0(k) + \boldsymbol{B}_0 u(k) + \boldsymbol{K}_0\boldsymbol{y}(k) \\ \hat{\boldsymbol{y}}(k) &= \boldsymbol{C}_0\boldsymbol{x}_0(k) \\ \hat{y}_r(k) &= \boldsymbol{C}_{0r}\boldsymbol{x}_0(k) \\ \boldsymbol{e}(k) &= \boldsymbol{y}(k) - \hat{\boldsymbol{y}}(k) \end{aligned} \tag{14}$$

where $(\boldsymbol{A}_0, \boldsymbol{B}_0, \boldsymbol{C}_0)$ is the identified nominal model of the plant $(\boldsymbol{A}, \boldsymbol{B}, \boldsymbol{C})$, $\boldsymbol{x}_0(k)$ an nx1 state, $\hat{\boldsymbol{y}}(k)$ an n_yx1 estimate of the plant output $\boldsymbol{y}(k)$, $\boldsymbol{e}$ the residual, and $\boldsymbol{K}_0$ the Kalman gain which minimizes the covariance of the estimation error $\boldsymbol{e}$.

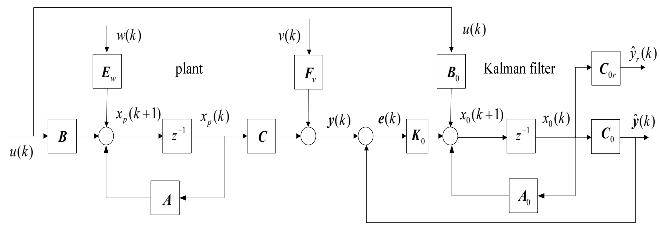

Fig. 3: Kalman filter and plant model driven by the residual

4.2 Residual and model-mismatch

In (Doraiswami & Cheded, 2012), the relation between the residual $e = y - \hat{y}$ and the KF inputs u and y was shown to be

$$e(z) = \frac{D_0(z)}{F_0(z)}\left(\Delta G(z)u(z) + \upsilon(z)\right) \tag{15}$$

The expression of the residual is employed to ensure high performance and stability of the soft sensor . The plant is re-identified whenever the residual exceeds some threshold. The residual will be a zero-mean white noise process if and only if there is no model mismatch.

Comment: The property of the residual (15) is exploited judiciously to ensure high performance and stability of the soft sensor in the face of model perturbation. The system is re-identified whenever the residual exceeds a prescribed threshold value. Further, the status of the system is also monitored in the process (Doraiswami & Cheded, 2012).

4.3 Augmented model of the plant and the Kalman filter

Let $(\boldsymbol{A}_{pk}, \boldsymbol{B}_{pk}, \boldsymbol{C}_{pk})$ denote the state-space model of the augmented plant formed of the plant itself $(\boldsymbol{A}, \boldsymbol{B}, \boldsymbol{C})$ and the KF $\left(\boldsymbol{A}_0 - \boldsymbol{K}_0\boldsymbol{C}, [\boldsymbol{B}_0\ \boldsymbol{K}_0], \boldsymbol{C}_0\right)$ relating the input $u(k)$ and the estimate of the inaccessible output $y_r(k)$. Let G_{pk} be the transfer function of the augmented state-space model $(\boldsymbol{A}_{pk}, \boldsymbol{B}_{pk}, \boldsymbol{C}_{pk})$, and G_{p0k} be the transfer function of the augmented nominal plant $(\boldsymbol{A}_{pk0}, \boldsymbol{B}_{pk0}, \boldsymbol{C}_{pk0})$ formed of the nominal plant $(\boldsymbol{A}^0, \boldsymbol{B}^0, \boldsymbol{C}_r^0)$ and the KF $\left(\boldsymbol{A}_0 - \boldsymbol{K}_0\boldsymbol{C}, [\boldsymbol{B}_0\ \boldsymbol{K}_0], \boldsymbol{C}_r\right)$.

5. EVALUATION ON A SIMULATED SYSTEM

The proposed scheme is evaluated on a DC servo motor. DC motors are versatile and extensively used in industry. Large DC motors are used in machine tools, printing presses, conveyors, fans, pumps, hoists, cranes, paper mills, textile mills, rolling mills, transit cars, locomotives, and so forth. Small DC motors are used primarily as control devices, such as servomotors for positioning and tracking. The DC motor system has two state variables namely the angular velocity $y_r = \omega$, and the armature current $y = i$. It is assumed that y_r is inaccessible and y is measured. The objective here is to estimate the angular velocity y_r of the DC motor using the KF which contains a copy of the identified plant model, that is driven by the error between the measured plant output y and its estimate $\hat{y}$, namely by the residual $y - \hat{y}$, and which generates the desired estimate $\hat{y}_r$ of y_r. As such, the soft sensor is in fact a Kalman filter which estimates the angular velocity y_r using the input u to the amplifier of the DC motor, and the armature current $y = i$. This current is measured using a static sensor which is inexpensive and which does not require any maintenance. The KF-based soft sensor designed here replaces the otherwise needed hardware velocity sensor (e.g. tachometer).

5.1 Off line identification

During the identification phase, it is assumed that the angular velocity y_r is measured (in practice, during the identification phase, the angular velocity may be measured using a physical tachometer). The plant model uncertainty is assumed to be the result of variations in the amplifier gain, the current sensor gain, and the tacho-generator gain.

The plant is identified by performing a number of experiments by varying the emulator parameters to mimic these variations. The emulator is chosen here to target only those model parameters that are likely to vary while in the case of the illustrated example(9), an unstructured emulator model was employed. Emulators are chosen to be static gains $\gamma_i : i = 1,2,3$. The gains γ_1, γ_2 and γ_3 are connected in cascade with the amplifier, the current sensor and the velocity sensor respectively as shown in Fig. 4.

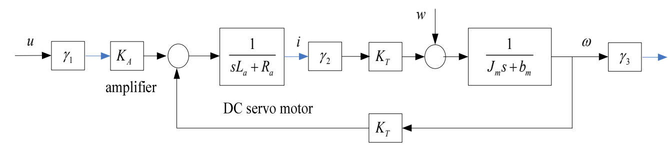

Fig. 4: Identification by varying the emulator parameters

5.2 Identified model of the plant

The identified nominal state-space model $(\boldsymbol{A}_0, \boldsymbol{B}_0, \boldsymbol{C}_0)$ was obtained using the subspace method, and the KF-based soft sensor was implemented using this identified model. The robustness of the soft sensor was evaluated by simulating perturbations in the actuator and the sensor by varying $\boldsymbol{B} = \boldsymbol{B}_0(1 + \Delta_B)$ and $\boldsymbol{C} = \boldsymbol{C}_0(1 + \Delta_C)$ respectively. Figure 5 shows the tracking performance and the status monitoring of the velocity control system. Subfigures A, C and E show respectively the output y_r and its estimate $\hat{y}_r$, while subfigures B, D and F show the auto-correlation of the residual $y_r - \hat{y}_r$ for different operating regimes: nominal, actuator perturbation and sensor perturbation.

Comments: Note that the estimates of the outputs are practically noise-free even though the 2 KF inputs, namely the current and control inputs are both noisy. The auto-correlation function of the residual visually enables us to distinguish the normal from abnormal operating conditions resulting from plant perturbations. A high system performance and stability is ensured by re-identifying the plant and re-designing the KF whenever the residual exceeds some threshold. This allows for vital tasks of performance monitoring and fault diagnosis to be realized, thus developing a fault tolerant system.

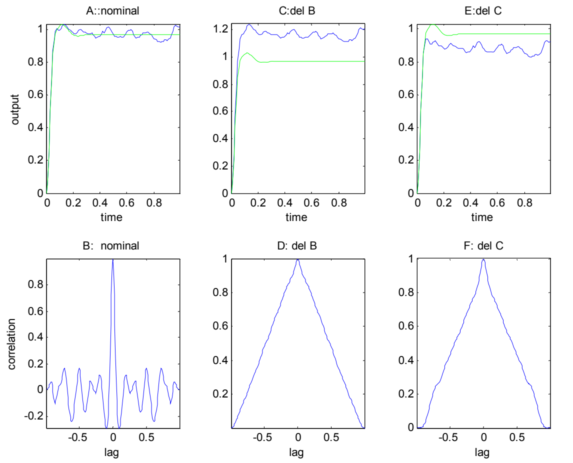

Fig. 5 The velocity, the current and the correlations

6. EVALUATION ON A PHYSICAL SYSTEM

The proposed scheme was evaluated on a laboratory-scale physical velocity control system in a similar way to that of the simulated system described earlier. The laboratory-scale physical DC motor interfaced to a personal computer using an analog-to-digital and a digital-to-analog converter, and its block diagram representation is similar to that given in Fig.4.

Fig. 6 shows the actual and estimated current and angular velocity plots. The subfigure on the top shows the current and its estimate while that on the bottom shows the velocity and its estimate. It can be deduced that the estimate of current and the angular velocity given by the KF-based soft sensor closely match those sensed by the current sensor and the tachometer, respectively. The noise spikes in the current are due to the intermittent break in the electrical contact between the rotating commutator and the brush. Note that the noise spikes are absent in the soft sensor velocity estimate.

7. CONCLUSION

In this paper, a proposed KF-based soft sensor was analysed, designed and successfully implemented on both a simulated and physical velocity control system. The reliable and accurate identification scheme of the plant using a number of parameter-perturbed experiments was made possible by the use of the powerful concept of emulators which were employed to mimic likely operating scenarios. This was a key aspect of our soft sensor design that ensures high performance and robust stability of the soft sensor in the face of model uncertainty and variation in the operating conditions. Further, as the identified model is reliable, it can then readily lead to the development of an effective model-based fault tolerant system. The KF plays a key role in providing a maintenance-free robust soft sensor.

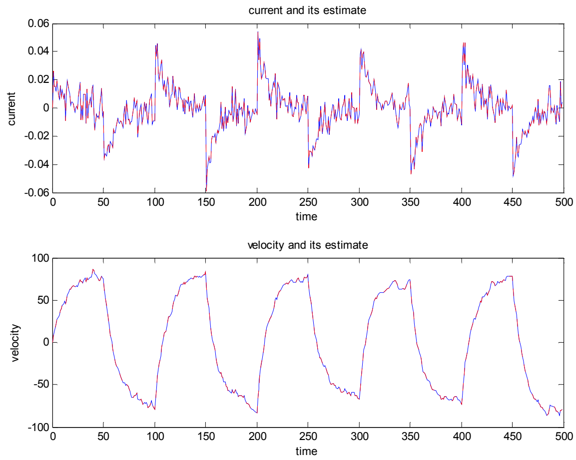

Fig.6. Velocity, current, and their estimates

REFERENCES

Angelov, P., & Kordon, A. (2010). Adaptive Inferential Sensors based on Evolving Fuzzy Models. *IEEE Transactions on Systems, Man and Cybernetics: Case Study* , 529-539.

Doraiswami, R., & Cheded, L. (2012). Kalman Filter for Fault Detection: an Internal Model approach. *IET Control Theory and Applications, 6*(5), 1-11.

Doraiswami, R., & Cheded, L. (2013). High Order Least Squares Identification: a New Approach. *ICINCO 2013: 10th International Conference on Informatics in Control, Automation and Robotics.* Reykjavik, Iceland.

Doraiswami, R., & Cheded, L. (2013). A Unified Approach to Detection and Isolation of Parametric Faults Using a Kalman Filter Residuals. *Journal of Franklin Institute, 350*(5), 938-965.

Fortuna, L., Graziani, S., & Xibilia, G. (2007). *Soft Sensors for Monitoring and Control of Industrial Processes.* Springer-Verlag.

Goodwin, G. C., Graeb, S. F., & Salgado, M. E. (2001). *Control System Design.* New Jersey, USA: Prentice Hall.

Kadlec, P., Gabrys, B., & S, S. (2009). *Data Driven Soft Sensors in the Process Industry* (Vol. 33). Computers and Chemical Engineering.

ACKNOWLEDGEMENT

The authors acknowledge the support of the department of Electrical and Computer Engineering, The University of New Brunswick, The National Science and Engineering Research Council (NSERC) of Canada, and the University of KFUPM, Saudi Arabia. The authors acknowledge Dr. Haris Khaled for his help and suggestions in the experimental work.